BMC Plant Biology

RESEARCH Open Access

The RAE1-STOP1 module regulates ABA sensitivity in early seedlings of Arabidopsis

Yuqing Zhang[1], Min Huang[1], Yinyin Liu[1], Mengmeng Yang[1], Yuqi Hou[1], Chao-Feng Huang[2], Ning Ning Wang[1] and Lei Li[1*]

Abstract

The SENSITIVE TO PROTON RHIZOTOXICITY 1 (STOP1) transcription factor plays a pivotal role in maintaining cellular ion balance and governing aluminum tolerance in plants. Abscisic acid (ABA) participates in aluminum tolerance by inducing the expression of several genes that are STOP1 targets. However, the interplay between ABA signaling and STOP1-mediated gene expression remains poorly understood. The F-box protein RAE1, an SCF-type E3 ligase component, recognizes STOP1 and controls its ubiquitination and degradation. This study revealed that exogenous ABA supplementation reduced STOP1 levels by promoting the expression of *RAE1*. Notably, both *RAE1* loss-of-function mutants and *STOP1* overexpressing lines showed enhanced sensitivity to exogenous ABA treatment, which correlated with early stage post-transcriptional upregulation of ABSCISIC ACID INSENSITIVE5 (ABI5). Our observations suggest that RAE1 operates as an ABA-responsive factor, exerting control over STOP1 homeostasis to regulate ABA responses in Arabidopsis. Interestingly, the *STOP1* dysfunctional alleles exhibit ABA sensitivity despite a reduction in ABI5, with similar expression levels of ABA-responsive genes, except for the ABI5 repressor MFT, compared to the *rae1* and STOP1 overexpression lines. This may suggest a bidirectional role of STOP1 in ABA sensitivity and highlights the critical importance of maintaining STOP1 homeostasis to balance growth and stress tolerance.

Single sentence summary

F-box protein RAE1 functions as an exogenous ABA responsive mediator to reduce STOP1 upregulation-mediated ABA sensitivity.

Keywords Arabidopsis, STOP1, Abscisic acid, Aluminum stress, RAE1, ABI5

*Correspondence:
Lei Li
lei.li@nankai.edu.cn
[1]Frontiers Science Center for Cell Responses, Department of Plant Biology and Ecology, College of Life Sciences, Nankai University, Tianjin 300071, China
[2]National Key Laboratory of Plant Molecular Genetics, Shanghai Center for Plant Stress Biology, CAS Center for Excellence in Molecular Plant Sciences, Chinese Academy of Sciences, Shanghai 200032, China

Introduction

The SENSITIVE TO PROTON RHIZOTOXICITY (STOP1) transcription factor is a key regulator of maintain cellular ion homeostasis [1–3]. STOP1 can regulate cellular organic acid and ion status by activating the expression of *Aluminum-activated Malate Transporter* (*ALMT1*), *CALCINEURIN B-LIKE INTERACTING PROTEIN KINASE23* (*CIPK23*) and *GLUTAMATE DEHYDROGENASE* (*GDHs*) which participate in malate secretion, ion transport and pH regulation-associated metabolism [3–5]. Specifically, STOP1 directly binds to the promoter of *nitrate transporter* (*NRT1.1*), promoting its transcriptional activation in response to low pH by enhancing nitrate uptake [6]. Owing to this essential role in cellular organic acid and ion homeostasis, STOP1 is regulated at the protein level via ubiquitination, SUMOylation, and phosphorylation. The F-box protein REGULATION of AtAlMT1 EXPRESSION 1 (RAE1), together with its isoform RAE1 HOMOLOG 1 (RAH1), aids the ubiquitination of STOP1 and controls its degradation through the 26 S proteasome [7]. The small ubiquitin-like modifier (SUMO) E3 ligase SAP AND MIZ1 DOMAIN- CONTAINING LIGASE1 (SIZ1) and SUMO protease EARLY IN SHORT DAYS4 (ESD4) all coordinately modulate the abundance and activity of STOP1 by participating in its SUMOylation and deSUMOylation [8, 9]. Moreover, MAP KINASE 4 (MPK4) positively controls STOP1 accumulation through its phosphorylation, which weakens its interaction with RAE1 and downregulates its degradation [10]. Cytokinin is reportedly involved in STOP1-mediated proton toxicity resistance [11]. Nevertheless, the interconnection between the STOP1-mediated ion homeostasis pathway and abscisic acid (ABA) remains uncertain with respect to the underlying mechanism and interaction.

ABA is a critical phytohormone that plays key roles in normal plant growth and development, as well as in integrating stress signals and responses throughout the plant life cycle [12]. ABA is involved in multiple plant developmental stages, including embryonic maturation, seed dormancy and germination, seedling establishment, leaf senescence and abscission, and plant responses to various biotic and abiotic stress conditions [13–16]. The major ABA signaling pathway consists of three core components: ABA receptors (PYRABACTIN RESISTANCE1 (PYR1)/PYR1-LIKE (PYL)/REGULATORY COMPONENTS OF ABA RECEPTOR (RCAR)), type 2 C protein phosphatases (PP2Cs), and sucrose nonfermenting1 (SNF1)-related protein kinase 2s (SnRK2s) [17–20]. When perceived by ABA receptors (PYR/PYL/RCAR), increased ABA levels can relieve the PP2Cs-mediated inhibition of downstream protein kinases, such as SnRK2s, leading to the phosphorylation of transcription factors (TFs) and altered expression of stress-responsive genes [21, 22]. Particularly, the basic leucine zipper (bZIP) TF ABSCISIC ACID INSENSITIVE5 (ABI5), is an important regulator of ABA signaling. Specifically, ABI5 is activated by phosphorylated SnRK2s and enhances the expression of ABA-responsive genes [15]. In turn, ABI5 can activate the expression of PP2Cs involving *ABI1* and *ABI2*, which function as a negative feedback in ABA signaling [23]. In addition, ABI5 promotes expression of *MOTHER OF FT AND FTL1* (*MFT*) which in turn supports early seedling development by repressing ABI5 expression in a feedback loop [24]. Moreover, ABI5 can alter the expression of ABA receptor *PYLs* in response to exogenous ABA treatment during seed germination [25]. ABI5-dependent central ABA signaling can therefore trigger both negative and positive feedback loops in ABA responses. Further, the ABA receptor can be post-transcriptionally regulated. Meanwhile, the protein kinase CYTOSOLIC ABA RECEPTOR KINASE 1 (CARK1) can phosphorylate the ABA receptor and positively regulate the ABA response [26, 27]. ABA signaling can help plants to cope with low pH by regulating genes involved in aluminum (Al) tolerance and detoxification [28–30]. For instance, in Arabidopsis, ABA induces the expression of *ALMT1*; however, an enhanced ABA-signaling mutant *abi1-1*, does not show changes in sensitivity to Al treatment [31]. Conversely, *abi5* mutants show increased sensitivity to Al stress, but are independent of *ALMT1* and *multidrug and toxic compound extrusions* (*MATE*) expression [32]. Similarly, the Al tolerance gene *Sensitive To Al Rhizotoxicity* (*OsSTAR1*) in rice is regulated by *STOP1 homolog* (*OsART1*) and members of the ASR (ABA-stress and ripening) gene family [33–35]. In contrast, toxic metals can lead to the accumulation of ABA in plant tissues, such as root tips, and the stimulation of ABA-responsive gene expression [29, 36–38]. Nonetheless, to date, the mechanisms underlying the interplay between ABA signaling and STOP1-mediated ion homeostasis remain largely unknown.

In this study, we observed that exogenous ABA treatment induced the expression of *RAE1*, leading to increased STOP1 degradation. Notably, *rae1* and *STOP1OE* plants exhibited enhanced sensitivity to exogenous ABA at the early seedling stage. This increased sensitivity was associated with the post-transcriptional upregulation of ABI5, a key TF involved in ABA signaling. These observations suggest the existence of an ABA-responsive RAE1-STOP1 module that reduces sensitivity to exogenous ABA treatment in Arabidopsis by preventing the increase of ABI5. Interestingly, the *STOP1* dysfunctional alleles exhibit ABA sensitivity despite reduced ABI5 levels, suggesting the existence of an alternative pathway in the absence of STOP1. This study reveals a bidirectional role of STOP1 in ABA sensitivity during the early seedling stage and underscores the

critical importance of maintaining STOP1 homeostasis in ABA signaling and response.

Results

Exogenous ABA treatment induces *RAE1* expression

Multiple ABA responsive element (ABRE) were identified in the promoter region of *rae1* gene (Fig. 1A). Moreover, publicly accessible transcriptome data in ePlants suggest that *RAE1* gene expression can be stimulated by ABA [39]. We further explored this through real-time quantitative PCR and GUS (β-glucuronidase) activity assay. Specifically, *RAE1* expression was significantly enhanced over a time course upon ABA treatment at 10 μM (Fig. 1B). GUS activity was measured in the root of 2 d old seedlings of a stable *pRAE1:GUS* Arabidopsis transformation line. The GUS signal significantly increased after treatment with ABA for 3 h (Fig. 1C-D). For long-term ABA treatment, from seed germination for up to 6 d, we observed enhanced GUS signals after ABA treatment at 1 μM (Fig. 1E). These results demonstrate that ABA induced the expression of *RAE1* in Arabidopsis. Additionally, GUS-staining revealed that *RAE1* was mainly expressed in the roots and veins of *Arabidopsis thaliana*.

The *rae1* mutant lines exhibit increased ABA sensitivity during the early seedling stage

To investigate whether *RAE1* is involved in the ABA response, we conducted an ABA sensitivity assay using three different *rae1* homozygous T-DNA insertion lines and their corresponding segregated wild type (WT) derived from the same heterogenous plants (Figure S1A-C). Although there was no change in seed germination in *rae1* mutant lines (Figure S1D, E), *rae1* seedlings showed a remarkably reduced proportion of greening cotyledons and fresh weight, compared with their corresponding WT counterparts (Fig. 2A-C). To confirm that the ABA-sensitivity phenotype was due to a *RAE1* mutation, we generated two complementation lines (*RAE1 CM14-1* and *RAE1 CM2-2*) of the *rae1-b* mutant and performed the same ABA sensitivity assays. ABA sensitivity in the *rae1* mutant lines was restored to the level of the wild type after complementation (Fig. 2A-C, Figure S2), indicating that *rae1* ABA-sensitive phenotype at the early seedling stage was indeed caused by a deficient *RAE1*. GUS-staining at the leaf development stage revealed that the expression of *RAE1* was mainly distributed in the veins (Figure S3A, C), but there was no apparent GUS-staining in the guard cells (Figure S3B). Therefore, no significant difference was observed in stomatal opening or water loss rate between the *rae1-b* mutant and WT under ABA treatment (Figure S3D-F). These results suggest that *RAE1* negatively regulated the ABA response, specifically at the early seedling stage.

Increased ABA sensitivity in *rae1* mutant lines is likely associated with elevated STOP1 levels

We hypothesized that the increased sensitivity of *rae1* mutants to ABA is associated with the upregulation of STOP1, a known RAE1 substrate. To test this hypothesis, we performed an ABA sensitivity assay using two *STOP1* overexpressing lines, *STOP1OE1* and *STOP1OE2*. As expected, both *STOP1* overexpressing lines displayed significantly increased sensitivity to ABA (Fig. 3A-C). A functional SCF (SKP1-CUL1-F-box) complex consists of SKP1 (ASK1), CULLIN 1 (CUL 1), RING-box 1 (RBX1), and F-box protein [40], and the interaction between F-box protein and ASKs is essential for SCF-type E3 ligase activity. To ascertain the potential enhancement of the interaction between ABA-induced RAE1 and ASK, we co-transformed *RAE1-cEYFP* and *ASK1-nEYFP* into Arabidopsis protoplasts and subjected them to ABA treatment. The fluorescence signal, which represents the interaction between RAE1 and ASK1, was significantly enhanced after ABA treatment (Figure S4A, B). Furthermore, an in vitro ubiquitination assay of STOP1 was performed in protoplasts extracted from WT and *rae1* plants with or without ABA treatment. This assay showed that ABA treatment increased STOP1 ubiquitination in the WT, but not in the *rae1-b* mutant (Fig. 3D). Subsequently, we treated both the *rae1-b* mutant and WT seedlings with ABA and assessed the resulting alteration in STOP1 protein levels to determine whether exogenous ABA triggers STOP1 degradation in plants. STOP1 protein abundance was measured in 7 d old seedlings after 2 d of ABA treatment. We found a significant reduction in STOP1 protein abundance in the WT, whereas no significant change was observed in the *rae1-b* mutant (Fig. 3E, F). Moreover, supplementation with the 26 S proteasome inhibitor MG132 reduced the STOP1 decrease caused by ABA treatment in the WT plants. Treatment with the protein synthesis inhibitor cycloheximide (CHX) is not performed due to its significant impact on early-stage development. These results suggest that ABA-induced degradation of STOP1 by RAE1 likely mediates the ABA response in seedlings.

Increased ABA sensitivity in *rae1* mutant lines is supported by the post-transcriptional upregulation of ABI5

STOP1 can regulate the cellular organic acid and ion status by activating the expression of *ALMT1*, *CIPK23* and *GDHs* which participate in malate secretion, ion transport, and metabolism associated to pH regulation [3, 4], possibly affecting ABA absorption. To investigate whether the increased sensitivity of *rae1* mutants to ABA was due to increased absorption of exogenous ABA through transporters regulated by STOP1, we used LC-MS to measure the ABA content in *rae1-b* and the corresponding WT after ABA treatment. No significant difference in ABA content was observed between *rae1-b* and the WT after ABA treatment (Figure S5A). Other

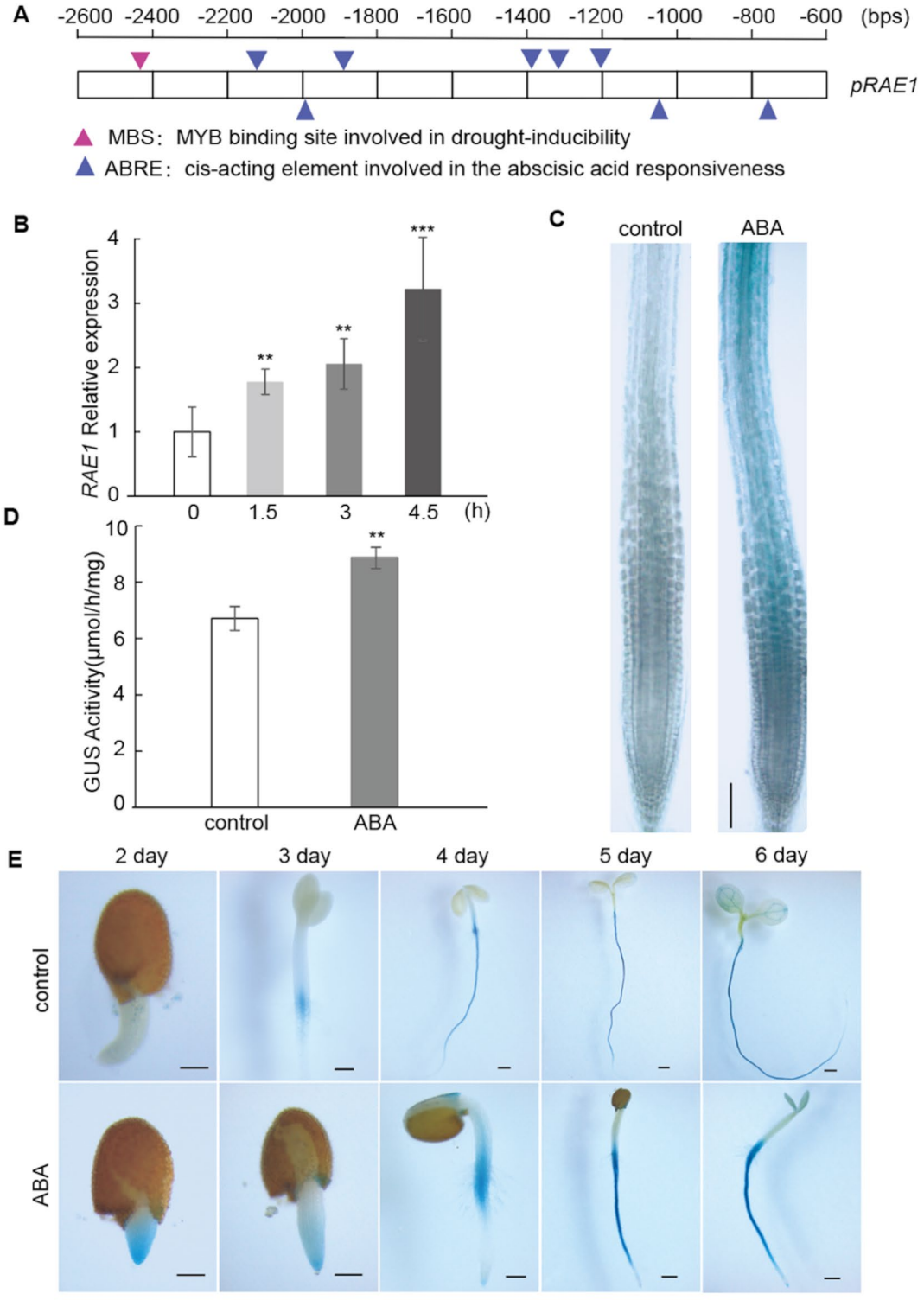

Fig. 1 ABA induced *RAE1* gene expression in Arabidopsis. (**A**) Cis regulatory elements in *RAE1* promoter (minus 2.6 kb) were analyzed by PlantCARE. ABRE and MBS elements in *RAE1* promoter are highlighted by colored arrows. (**B**) The relative expression of *RAE1* in 7 d old plate grown Arabidopsis seedlings in response to ABA treatment are shown as column graphs. The level of *RAE1* transcripts after a time course of 10 μM ABA treatments (0, 1.5, 3, 4.5 h) were determined by qRT-PCR. (**C**) GUS-stained root tips from 5 d old seedlings of an Arabidopsis line with stable expression of *pRAE1: GUS* were treated with or without 10 μM ABA treatment for 3 h for short-term ABA response analysis (scale bar = 100 μm). (**D**) GUS activity was determined in 2 d old seedlings of the *pRAE1: GUS* line with or without 10 μM ABA treatment. (**E**) GUS stained 2 to 6 d old seedlings of the *pRAE1: GUS* line with or without 1 μM ABA treatment from seeds (scale bar = 200 μm). Error bars represent the standard deviation for four biological replicates for qRT-PCR and GUS activity assay (* indicates significant difference ($P < 0.05$), ** indicates highly significant difference ($P < 0.01$), as per Student's *t*-test)

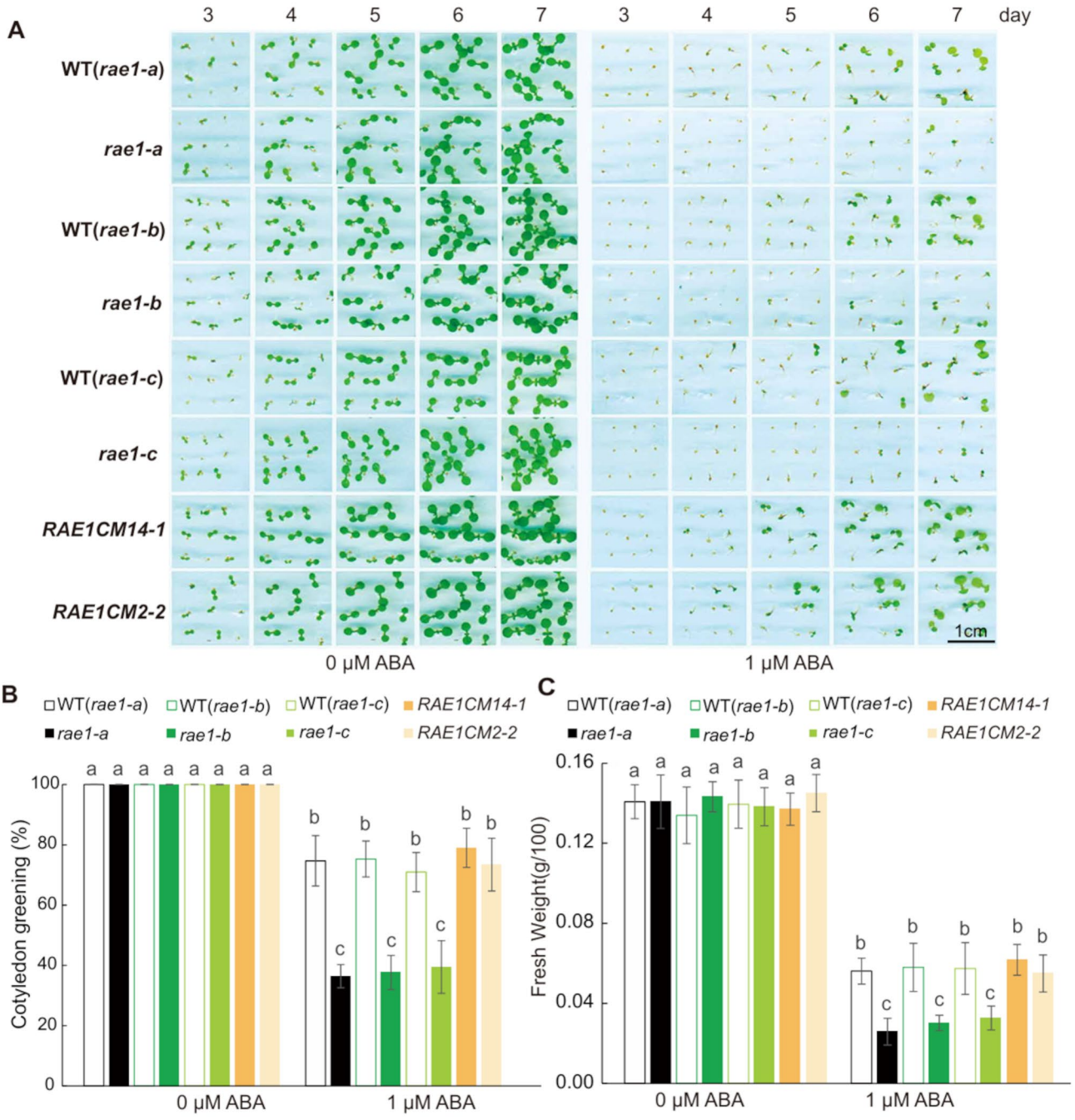

Fig. 2 RAE1 loss of function leads to increased sensitivity to exogenous ABA treatment at the early seedling stage. (**A**) Seeds of *rae1-a*, *rae1-b*, rae1-c, their corresponding segregated wild type, and two complementation lines (*RAE1CM14-1* and *RAE1CM2-2*) were cultivated on half-strength MS medium with or without 1 μM ABA treatment. Photographs capturing representative images of seedlings aged between 3 and 7 d were taken daily and subsequently presented. (**B-C**) The proportion of 7 d old seedlings with cotyledon greening and fresh weight are shown as column graphs. Error bars represent the standard deviation for three representative plates. Grouping was determined by one-way ANOVA ($P < 0.05$, Duncan's multiple-range test)

phytohormones, including indole-3-acetic acid (IAA), salicylic acid (SA), and jasmonic acid (JA), were also measured but no significant differences were observed (Figure S5B, C, D). To explore whether the increased ABA sensitivity observed in *rae1* mutants was influenced by *ALMT1*, which is a target gene of STOP1 and highly induced in *rael-b* (Figure S7C, Data S4), we tested the ABA sensitivity of *ALMT1* overexpressing and mutant lines. The results showed that the sensitivity to ABA in both the *ALMT1* overexpressing lines and *almt1* mutant lines was similar to that in the WT (Figure S6A, B).

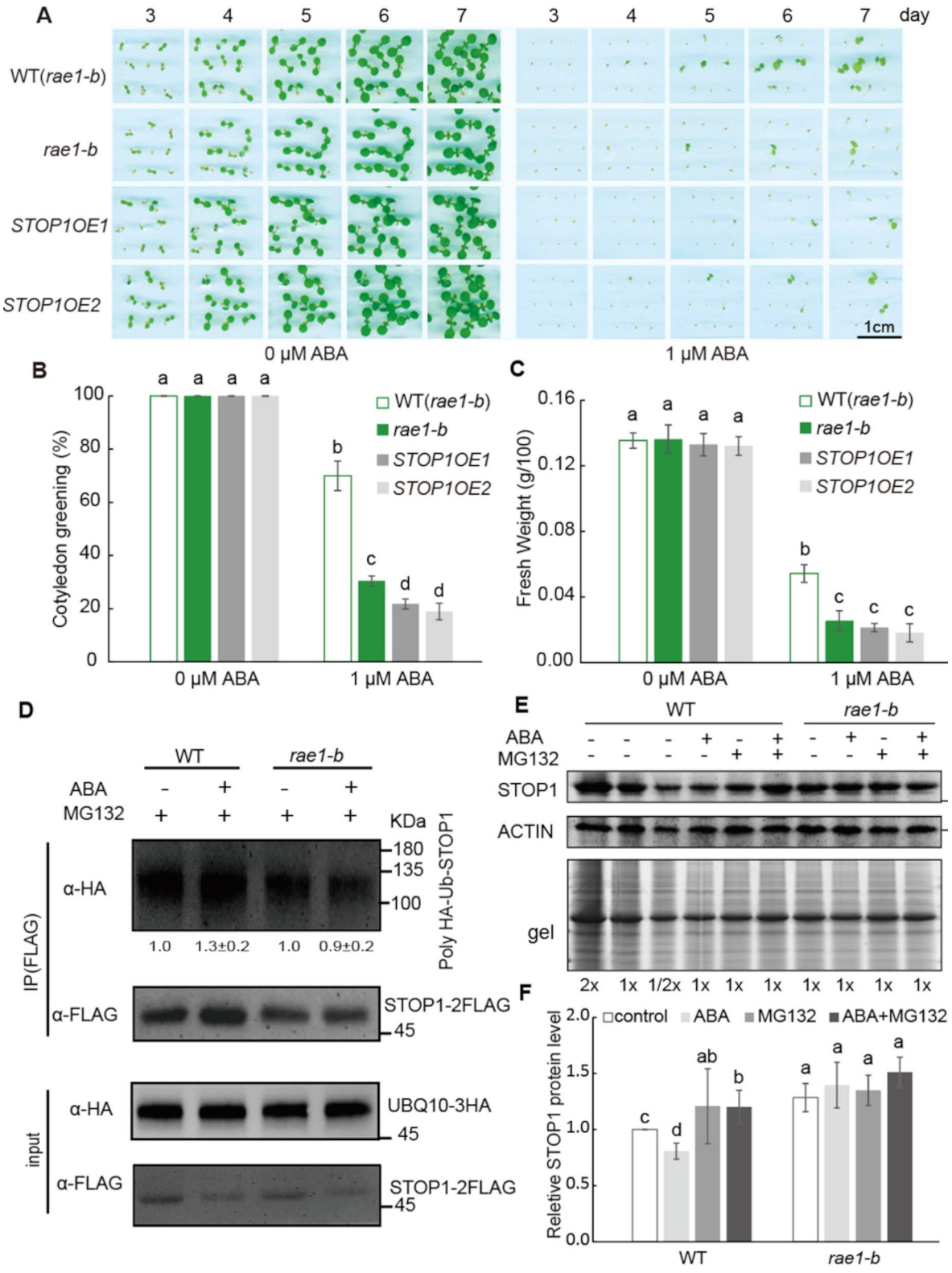

Fig. 3 (See legend on next page.)

(See figure on previous page.)

Fig. 3 *STOP1* overexpression caused increased ABA sensitivity comparable to *rae1* at the early seedling stage. (**A**) Seeds of *rae1-b*, its corresponding segregated wild type, and two STOP1 overexpressing lines (*STOP1OE1* and *STOP1OE2*) were cultivated on half-strength MS medium with or without 1 μM ABA treatment. Photographs capturing representative images of seedlings aged between 3 and 7 d were taken daily and subsequently presented. (**B-C**) The proportion of 7 d old seedlings with cotyledon greening and fresh weight are shown as column graphs. Error bars represent the standard deviation for three representative plates. Grouping is determined by one-way ANOVA ($P < 0.05$, Duncan's multiple-range test). (**D**) ABA treatment increased the level of STOP1 ubiquitination in WT but not in *rae1-b* protoplasts. Two pHBT expression vectors containing either *35 S: STOP1-2FLAG* or *UBQ10-3HA* were co-transformed into protoplasts extracted from WT or *rae1-b* Arabidopsis leaves and incubated with or without ABA/MG132 treatments. STOP1 was enriched from total protein using α-FLAG beads. Western blot analysis was performed to determine the abundance and ubiquitination of the enriched STOP1 using antibodies against HA/Flag. The numbers below the blotting indicate the relative level of STOP1 ubiquitination in either WT or *rae1-b* with or without ABA treatment (± SD for three biological replicates). (**E**) ABA treatment induced STOP1 reduction in WT but not in *rae1-b* mutants, which can be abolished by proteasome inhibitor MG132. 7 d old Arabidopsis seedlings grown on half-strength MS medium were transferred to new plates with or without 10 μM ABA and grown for another 2 d. Seedlings under control and ABA treatment were treated with or without 50 μM MG132 for another 6 h. Western blot of SDS-PAGE separated total protein was performed using an antibody against STOP1. Actin blotting and Coomassie blue stained gel were used for equal loading. A gradient of total protein at double, single and half amount (2x/1x/1/2x) were utilized in wild type to avoid overexposure in western blotting. (**F**) STOP1 signal from blotting was determined using ImageJ and is represented in column graphs. Grouping was determined by Student's *t*-test ($P < 0.05$). Error bars represent the standard deviation for three biological replicates

To characterize the enhanced ABA-sensitive *rae1* phenotype, we performed RNA-seq analysis on *rae1-b* and WT seedlings after ABA treatment. All the genes measured in the transcriptomic data are presented as volcanic plots (Figure S7A, Data S1). Principal component analysis (PCA) shows a clear clustering of biological triplicates and a distinct separation of *rae1-b* from the wild type (Fig. 4A). A total of 22,629 genes were identified among these data, 211 which were marked in red for significant up-regulation in *rae1-b* mutants, while 206 genes were marked in blue for significant down-regulation in *rae1-b* mutants (Figure S7A, Data S1). Notably, the activation and repression of ABA-positive and ABA-negative regulatory factors were prevalent in *rae1-b* mutants (Fig. 4B-C, Data S2, S3). Although *ABI5* transcript levels did not differ between *rae1-b* mutants and the WT, ABI5 downstream genes, such as *EARLY METHIONINE-LABELLED 6* (*EM6*), *RESPONSIVE TO ABA 18* (*RAB18*), *RESPONSIVE TO DESICCATION 29B* (*RD29B*), and *MOTHER OF FT AND TFL1* (*MFT*), were significantly upregulated in *rae1-b* compared with the WT (Fig. 4C, Data S3), indicating a potential post-transcriptional upregulation of ABI5 in *rae1*. To test this hypothesis, we used an antibody against ABI5 to determine and compare the abundance of ABI5 in *rae1-b*, *STOP1* null allele-*stop1-2* [41] and *STOP1* overexpression line-*STOP1OE1* [42]. Compared with the WT, the abundance of the ABI5 protein was higher in *rae1-b* and *STOP1OE1*, and lower in *stop1-2*, regardless of ABA treatment (Fig. 5A, B). Furthermore, we generated an *abi5-8::rae1-b* double mutant by crossing *rae1-b* with *abi5-8* and performed an ABA sensitivity assay (Fig. 5C-E). The introduction of *abi5-8* significantly reduced ABA sensitivity in *rae1-b*. In contrast, the introduction of *cark1*, a kinase that activates the ABA receptors PYL8 and PYR1 by phosphorylation [26], did not diminish the ABA sensitivity phenotype in *rae1-b*. This observation implies that the ABA-sensitive trait in *rae1* was likely influenced by ABI5.

The post-transcriptional upregulation of ABI5 in the *rae1* mutant may be attributed to its reduced degradation. Therefore, it is a question whether ABI5 is a target of RAE1-mediated ubiquitination. In addition, STOP1 can possibly interact with ABI5 to modulate its stability and functionality. However, yeast two-hybrid and Bimolecular fluorescence complementation (BiFC) experiments suggested no direct interaction between ABI5 and either RAE1 or STOP1 (Figure S8A, B). While a direct interaction between RAE1-ABI5 or STOP1-ABI5 is not supported by experiments, the relative expression of reported factors associated with ABI5 degradation was extracted from RNA sequencing data (DataS3). These ABI5 regulatory factors involve *DWD hypersensitive to ABA1/2* (*DAW1/2*), *KEEP ON GOING* (*KEG*), *PLANT U-BOX 8/35* (*PUB8/35*), *SAP AND MIZ1 DOMAIN-CONTAINING LIGASE1* (*SIZ1*), *ABI FIVE BINDING PROTEIN1* (*AFP1*), *ABA-hypersensitive DCAF1* (*ABD1*), *for XPO1-interacting WD40 protein 1* (*XIW1*), *MYB30-INTERACTING E3 LIGASE 1* (*MIEL1*), *REPRESSOR OF UV-B PHOTOMORPHOGENESIS 1/2* (*RUP1/2*), *DAMAGED DNA BINDING PROTEIN1A/B* (*DDB1A/B*), *DDB1-CUL4 ASSOCIATED FACTOR 1* (*DCAF1*), *CULLIN4-based E3* (*CUL4*), *Receptor for Activated C Kinase 1 A/B/C* (*RACK1A/B/C*) [43–53]. Notably, the expression levels of *ABD1*, *DDB1B*, *RACK1B*, and *RACK1C* were reduced, whereas the expression of *MIEL1* increased (Fig. 4C, Data S3).

ABA sensitivity in *STOP1* overexpression and dysfunctional lines

A reduction in ABI5 protein levels in the *stop1-2* mutant (Fig. 5A-B) could potentially lower its sensitivity to exogenous ABA treatment. To investigate this, we assessed the ABA sensitivity of the *stop1-2* mutant alongside the *rae1-b* mutant and compared them with wild-type plants (Fig. 6A, B). Interestingly, while *rae1-b* exhibited the highest sensitivity to exogenous ABA, *stop1-2* unexpectedly showed an increased sensitivity to ABA compared

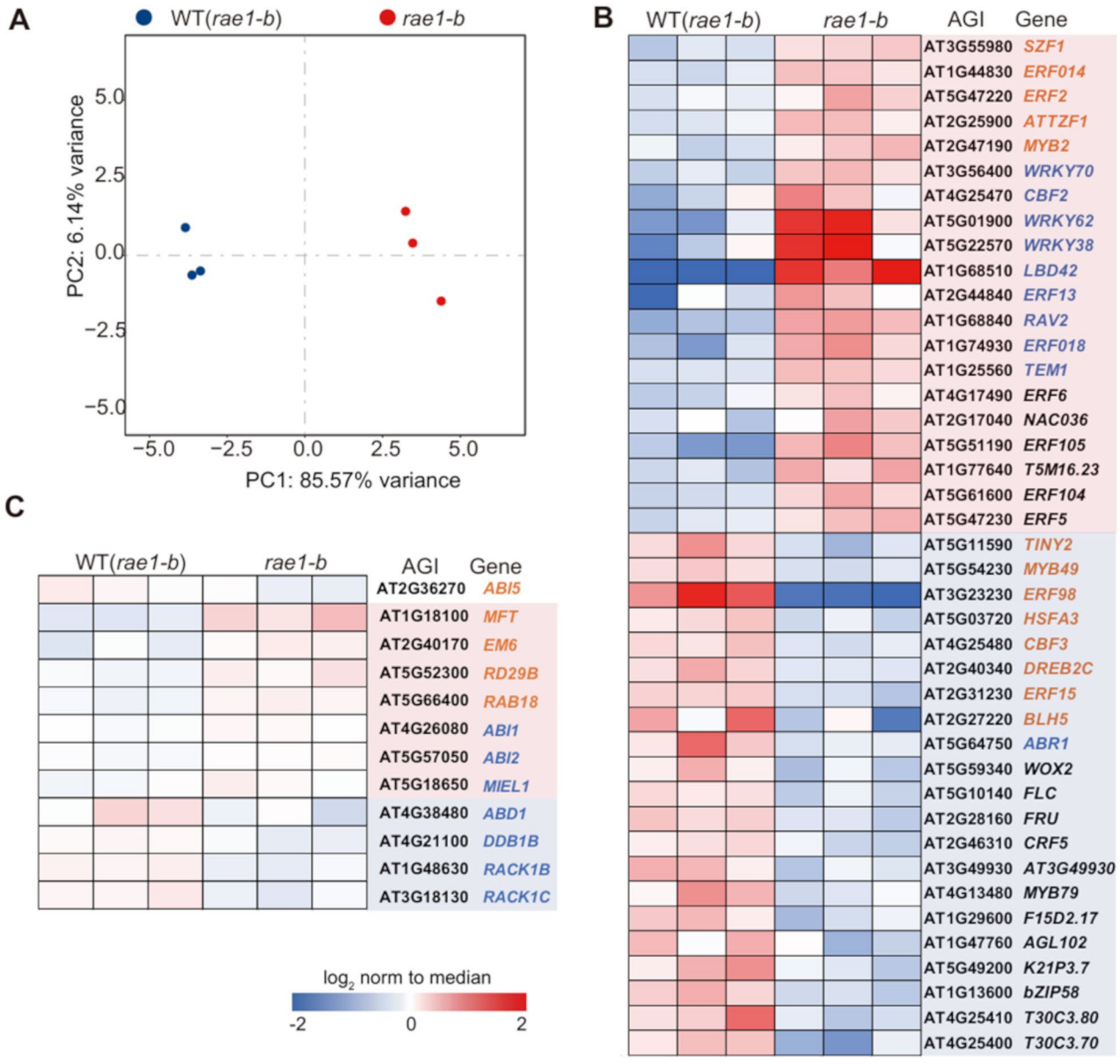

Fig. 4 Alterations in gene expression of ABA-associated transcription factors and regulatory genes in *rae1-b*. (**A**) Principal component analysis (PCA) was conducted using the transcript levels of all measured genes in wild type (WT) and *rae1-b*. PC1 and PC2 values are represented on the x and y axes, respectively. RNA-seq was performed using total RNA extracted from seven-day-old Arabidopsis seedlings treated with 10 μM ABA for three hours (DataS1). (**B**) Heatmap displaying transcription factors with significant expression changes (fold change > 1.5 or < – 1.5, $P < 0.05$) in *rae1-b* compared to WT (DataS2). (**C**) Heatmap illustrating significant expression changes in ABA response genes, including downstream targets of ABI5 (*MFT*, *EM6*, *RD29B*, and *RAB18*) and PP2C family members (*ABI1*, *ABI2*) in *rae1-b*. The expression level of *ABI5*, ABI5 E3 ligase and proteins associated with ABI5 degradation (*MIEL1*, *ABD1*, *DDB1B*, *RACK1B/C*), are also shown. Genes which were characterized as ABA positive regulators/ABI5 targets were colored in orange fonts, negative regulators were colored in blue fonts

to wild-type plants. This heightened ABA sensitivity in *stop1-2* was further corroborated by the upregulation of ABI5 target genes, including *EM6*, *RAB18*, and *RD29B*, along with central ABA signaling feedback genes *ABI1* and *ABI2* in *stop1-2* (Fig. 6C-I). These genes exhibited similar expression levels across the *rae1-b*, *stop1-2*, and *STOP1OE2* lines, suggesting that the *STOP1* null allele can activate ABA perception and/or signaling despite a reduction in ABI5 protein abundance. However, *MOTHER OF FT AND TFL1* (*MFT*), a known target of ABI5 that directly repress *ABI5* expression [24], was induced only in the *rae1-b* and *STOP1OE2* lines, but not in *stop1-2* (Fig. 6F). Additionally, the ABI5 target gene *RAB18* showed reduced expression in *stop1-2* under

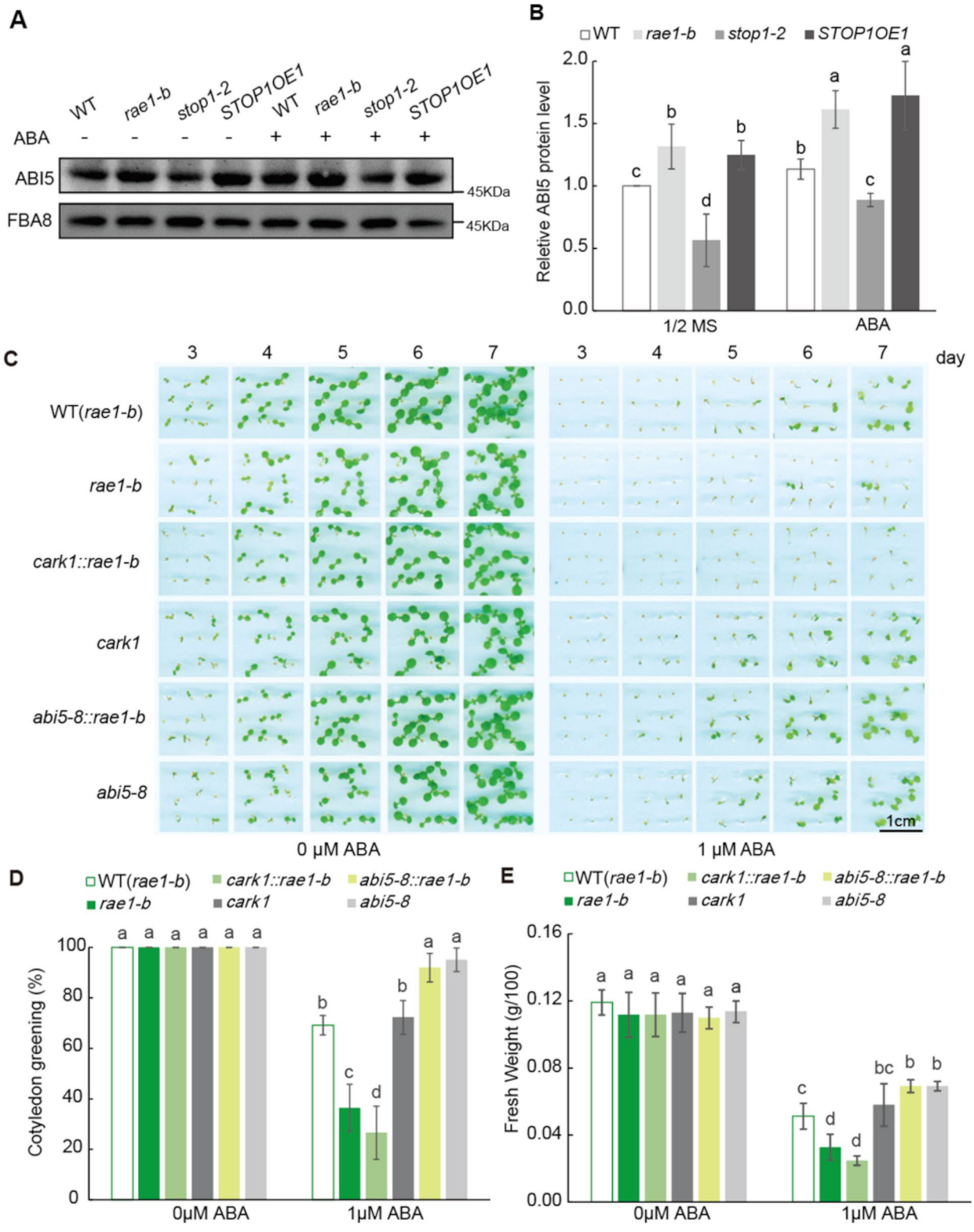

Fig. 5 (See legend on next page.)

(See figure on previous page.)

Fig. 5 Heightened ABA sensitivity in *rae1* correlates with ABI5, not CARK1. (**A**) The abundance of ABI5 protein increased in *rae1-b* and *STOP1OE1*, but decreased in *stop1-2*, regardless of ABA treatment. 5-d old Arabidopsis seedlings (WT, *rae1-b*, *stop1-2*, and *STOP1OE1*) were transferred to fresh plates with or without 10 μM ABA and grown for 20 h. Total protein was separated by SDS-PAGE, followed by Western blotting with an antibody against ABI5. FBA8 was used as a control for equal loading. Grouping is determined by a Student's *t*-test ($P < 0.05$). Error bars represent the standard deviations for five biological replicates. (**B**) ABI5 Western blotting signals are normalized to WT and presented as column graphs. Error bars represent the standard deviation for five biological replicates. (**C**) Mutant lines (*rae1-b*, *cark1*, *abi5-8*, *abi5-8::rae1-b*, *and cark1::rae1-b*) and WT were grown on half-strength MS medium with or without 1 μM ABA treatment. Daily photographs of seedlings aged between 3 and 7 d are shown (**D-E**) Column graphs depict the proportion of 7 d old seedlings with cotyledon greening and their fresh weight. Error bars represent the standard deviation for three representative plates. Grouping was determined by one-way ANOVA ($P < 0.05$, Duncan's multiple-range test)

control condition (Fig. 6I). These findings suggest that the mechanisms underlying heightened ABA sensitivity differ between the *rae1-b/ STOP1OE2* lines and *stop1-2*.

The increased ABA sensitivity observed in *STOP1* upregulation lines (*rae1-b* and *STOP1OE2*) and *STOP1* knockout (*stop1-2*) suggests a possible bidirectional role of STOP1 in regulation of ABA sensitivity. To explore potential alternative regulatory pathways of STOP1, we have analyzed the relative expression of bZIP transcription factors ABF1 and ABF3, subclass II and III SnRKs (*SNRK2.3* and *SNRK2.8*) which were found to be responsive to various stresses in *stop1-2* knockout mutant [54]. All these four genes show upregulation at transcription in tested lines compared with WT under exogenous ABA treatment (Figure S11). *ABF1* shows the highest expression in *stop1-2* compared to all other lines.

To validate and further explore RAE1-STOP1 module in ABA sensitivity, we tested the ABA sensitivity of the *RAE1* overexpression line *RAE1OE1*, point mutation *rae1-1* (G167R), *stop1-3* (H352Y) and *rae1-1::stop1-3* double mutant lines all in a WT(A30) genetic background. The WT(A30) is a *pAtALMT1:LUC* reporter line established in Col-0 [55]. All lines in the WT(A30) background exhibited slightly increased ABA sensitivity. Therefore, we performed an ABA treatment under a concentration range (0.25-1 μM) to disentangle the relationship between RAE1 and STOP1 in conferring ABA sensitivity (Figure S9A-B). As expected, the *RAE1OE1* line exhibited slightly but significantly reduced ABA sensitivity, which was further supported by qPCR analysis showing downregulation of the ABI5 target gene *RD29B* (Figure S9C-F). Notably, the sensitivity of the *rae1-1::stop1-3* double mutant was higher than that of the two single mutants under 0.25 and 0.5 μM ABA treatment. This suggests a possible synergistic effect on ABA sensitivity in the double mutant.

The bidirectional sensitivity to exogenous ABA treatment in *STOP1* upregulation and dysfunctional alleles prompted us to investigate osmotic treatment mimicking drought conditions during the early seedling stage. An obvious reduction in osmotic stress tolerance was observed in *STOP1* null allele *stop1-2*, but not in other tested lines (Figure S10A-C). A previous report also found that *STOP1* dysfunctional allele was sensitive to drought and salt treatment [3]. In this study, we found that *RAE1* expression was induced by exogenous ABA treatment and reduced in *ABI5* dysfunctional alleles, but its expression was downregulated by high salt treatment, probably serves to prevent STOP1 reduction. This result suggests that the upregulation of STOP1, either by *RAE1* knockout or *STOP1* overexpression, confers increased sensitivity to exogenous ABA treatment but not to osmotic or salt stresses during the early seedling stage.

Discussion

The SCF-type E3 ligase F-box protein RAE1 downregulates STOP1 levels by enhancing its ubiquitination and subsequent degradation. Further, *RAE1* expression is induced by Al treatment and is dependent on STOP1 [55]. However, whether phytohormones regulate the RAE1-STOP1 module for cellular ion homeostasis or other responses remains unclear. In this study, we characterized RAE1 as an ABA-responsive mediator that contributes to lower ABA sensitivity associated with STOP1 at the early seedling stage. Indeed, *RAE1* expression was induced by exogenous ABA treatment and was mainly distributed in the vein tissues (Fig. 1C, D). Consistently, exogenous ABA treatment enhanced the expression of *RAE1* and the formation of a functional SCF complex that ubiquitinated STOP1 and lowered its abundance at the early seedling stage (Fig. 3, Figure S4). Moreover, *rae1* mutants exhibited increased ABA sensitivity, while the *RAE1* overexpression line showed reduced ABA sensitivity during early seedling development (Fig. 2, Figure S9A-C). Further, *STOP1* overexpressing lines were similar to the *rae1* lines in terms of ABA sensitivity (Fig. 3A-C), suggesting that their increased ABA sensitivity was associated with the RAE1-STOP1 module. Furthermore, ABA and other phytohormones remained at the same level in *rae1* as in WT seedlings (Figure S5), indicating that the absorption of exogenous ABA or other phytohormones was not the cause. To determine whether this was associated with known STOP1 target genes, we further investigated *ALMT1* for its involvement in ABA sensitivity (Figure S6). However, the *almt1* knockout and overexpressing lines were similar to the WT plants under ABA treatment, indicating that the *rae1* ABA-sensitive phenotype cannot be explained by the known STOP1-ALMT1 pathway.

Additionally, we conducted a transcriptome analysis of *rae1-b* and compared it with that of the WT under ABA treatment to determine what genes participating in the

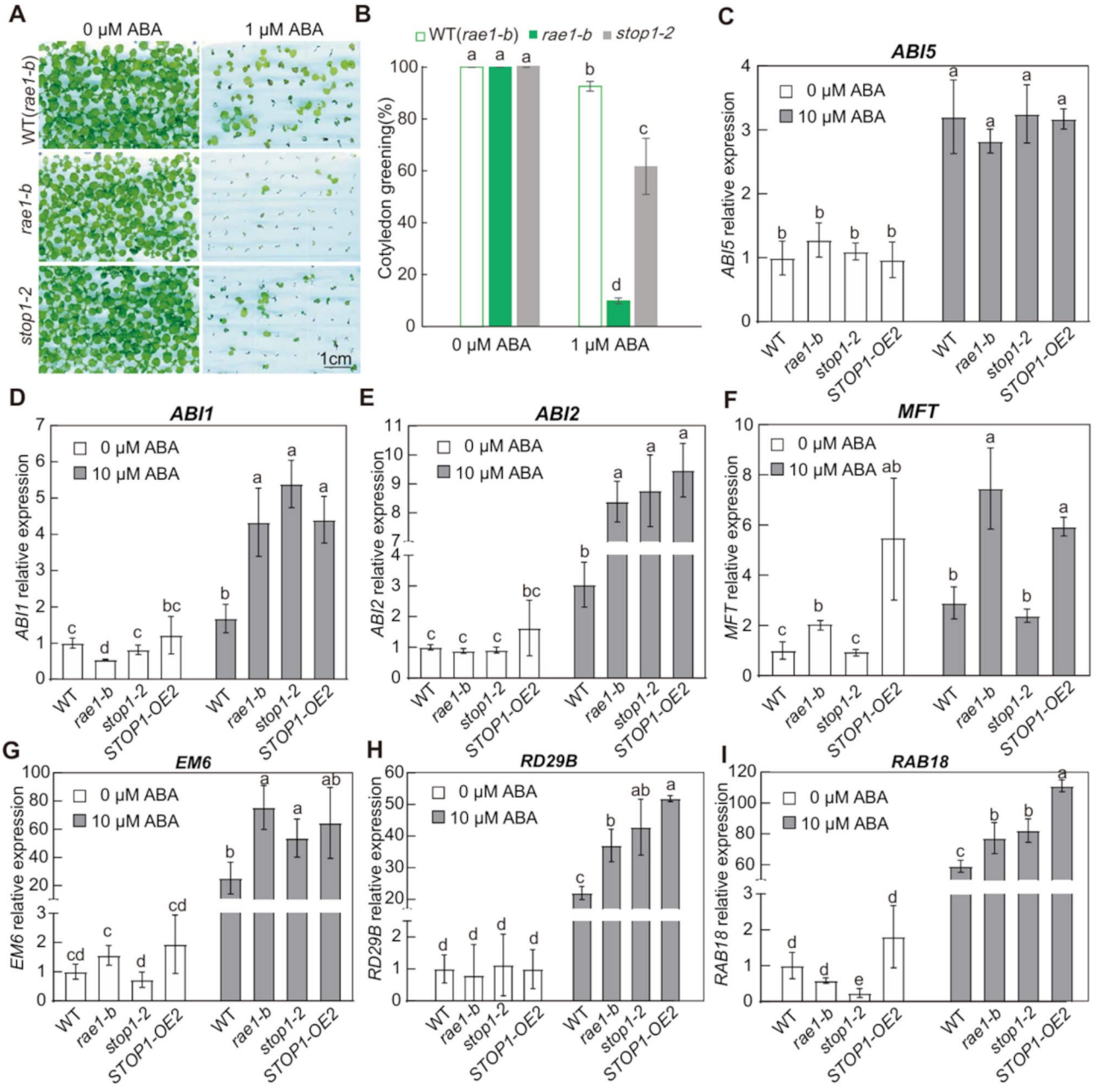

Fig. 6 Differential sensitivity to exogenous ABA treatment in *rae1-b* and *stop1-2* mutants indicated by varied *MFT* expression. **(A)** Seeds of *rae1-b*, *stop1-2*, and wild type were cultivated on half-strength MS medium with or without 1 μM ABA treatment. Representative images of 9-day-old seedlings are shown. **(B)** The proportion of 9 d old seedlings with cotyledon greening are shown as column graphs. Grouping is determined by one-way ANOVA ($P < 0.05$, Duncan's multiple-range test). Error bars represent the standard deviation across three representative plates. **(C-I)** Seven-day-old Arabidopsis seedlings (*WT*, *rae1-b*, *stop1-2*, and *STOP1OE2*) grown on plates were transferred to new plates with or without 10 μM ABA and incubated for three hours. Gene expression of *ABI5*, *ABI1*, *ABI2*, *MFT*, *EM6*, *RD29B*, and *RAB18* was quantified by qRT-PCR. Relative expression levels, normalized to WT under control conditions, are shown as column graphs. Error bars represent the standard deviation for biological triplicates. Grouping is determined by a Student's *t*-test ($P < 0.05$)

ABA response are regulated by RAE1 (Fig. 4A, Figure S7A). Changes in the transcript levels of ABA-positive and-negative regulatory factors were prevalent in *rae1-b* (Fig. 4B, Data S2), suggesting that the strong ABA response in *rae1-b* was a combined effect of positive and negative regulatory pathway factors in ABA signaling. This finding was consistent with previous reports suggesting that ABI5 not only functions as an important regulator of ABA signaling, but can also activate the expression of *ABI1* and *ABI2,* and change the expression pattern of ABA receptor PYLs, which

function as a feedback of central ABA signaling [23, 25, 56]. Notably, whereas two negative regulator PP2Cs genes and other known ABI5 target genes increased at the transcript level, there was no change in *ABI5*, which suggest a post-transcriptional control of ABI5. As expected, ABI5 protein levels increased in both the *rae1* mutant and *STOP1* overexpressing lines, but decreased in *stop1-2* (Fig. 5A, B). Moreover, the ABA sensitive phenotype *rae1-b* was fully restored by the *ABI5* null allele *abi5-8* (Fig. 5C-D). Altogether, these data indicate that the *rae1-b* ABA sensitive phenotype was most likely through the ABI5-mediated ABA responses.

The expression levels of several genes encoding reported ABI5 degradation regulatory factors changes. These involves reduced expression of *ABD1*, *DDB1B*, *RACK1B*, and *RACK1C*, but increased expression of *MIEL1* (Fig. 4C, Data S3). ABD1 and DDB1 function together in a CULLIN4-based E3 ubiquitin ligase complex to promote ABI5 degradation during early seedling stage [48]. RACK1 facilitates ABI5 degradation, while activated ABI5 can inhibit *RACK1* gene expression [53]. MIEL1 can ubiquitinate ABI5 and facilitate its degradation during gemination [49]. Increased expression of *MIEL1* may help to downregulate ABI5 protein level as a response of ABI5 accumulation. Changes in expression of genes encoding ABI5 regulatory factors may contribute to ABI5 deficient degradation and accumulation in the *rae1-b* mutant, but could also be a consequence of ABI5 accumulation, as seen with *RACK1* genes, *ABI1* and *ABI2*. In addition, Gene Ontology (GO) analysis revealed a substantial extent of upregulation of transporters and ubiquitin-related genes in the SCF complex of the *rae1-b* mutant (Figure S7B, C). Among them, several F-box-related genes were significantly upregulated (Figure S7D, Data S5), particularly the homologous gene *RAH1*, which is closely associated with *RAE1*. This wide-scale transcriptome response to RAE1 defects suggests the presence of a complicated network that maintains cellular ion homeostasis through STOP1 and its crosstalk with other regulators of plant signaling involving ABA. However, a direct interaction between ABI5 and RAE1 or STOP1 was not demonstrated. To date, the exact mechanism by which RAE1 or STOP1 regulates the increase in ABI5 protein remains unclear.

A seemingly contradictory observation is that the *stop1-2* mutant exhibits increased sensitivity to ABA despite a reduction in ABI5 protein levels (Figs. 5 and 6). This was further confirmed in a *STOP1* point mutation allele, *stop1-3* (Figure S9A-B). An in-depth analysis of ABA-responsive genes and ABI5 targets corroborated this heightened ABA sensitivity in *stop1-2*. However, the ABI5 target and repressor MFT was induced only in the *rae1-b* and *STOP1OE2* lines, but not in *stop1-2* (Fig. 6F), suggesting that the mechanisms underlying the heightened ABA sensitivity differ between the *STOP1* upregulation line and *STOP1* knockout line. This was also supported by the observation of a synergistic effect on ABA sensitivity in the *rae1-1::stop1-3* double mutant (Figure S9A-B). The loss of STOP1 function triggers a reorganization of multiple transporters, transcription factors, and other regulatory components [1, 4–6, 41], potentially altering ABA perception and signaling. A bZIP transcription factor ABF1 shows the highest expression in *stop1-2* compared with WT and STOP1 upregulation lines (Figure S11). ABFs were found to stimulate ABA responsive gene expression [23], and may serve as alternative regulators of ABA sensitivity in the *stop1-2* mutant when ABI5 level is reduced. Although the specific mediator(s) responsible for activating ABA perception and/or signaling in STOP1 dysfunctional alleles remains unresolved in this study, the observation that both STOP1 upregulation and loss-of-function mutants exhibit enhanced ABA sensitivity suggests a potential bidirectional role of STOP1 protein homeostasis in ABA perception and signaling. This also underscores the necessity of the ABA-responsive RAE1 in preventing STOP1 accumulation, which can lead to an increase in ABI5 and heightened ABA sensitivity, ultimately inhibiting early seedling development. Despite the common increased sensitivity to exogenous ABA treatment in both *STOP1* upregulation and dysfunctional alleles, only *STOP1* dysfunctional alleles were found to confer increased sensitivity to osmotic stress (Figure S10A-B) and salt stress as reported previously [3]. Noticeably, *RAE1* expression was reduced in response to salt treatment, possibly serving to maintain STOP1 protein levels for salt stress tolerance.

A hypothetical working model of RAE1 as an ABA-responsive factor that attenuates ABA signaling is schematized in Fig. 7. This model proposes a link between exogenous ABA treatment and STOP1 through RAE1, which is characterized with ABI5 protein level change, suggesting that the STOP1 protein level must be precisely regulated to coordinate stress resistance and growth. This model is expected to provide clues to investigate the crosstalk between endogenous ABA signaling and STOP1 mediated stress responses. On the other hand, the increased ABA sensitivity of *rae1-1* upon introducing the *stop1-3* dysfunctional allele suggests that STOP1 accumulation might not be the sole contributor to ABA sensitivity in *rae1* mutant lines. RAE1 was recently reported to interact with another transcription factor RHD6 to promote its degradation [5]. It is highly likely that the F-box protein RAE1 may target other mediators (referred to as X), in addition to the known RAE1-STOP1 module, to confer ABA sensitivity. Although no new RAE1 targets were identified in this study, we believe the observed synergistic ABA sensitivity in double mutant provide a foundation for future studies aimed at identifying these new X protein(s).

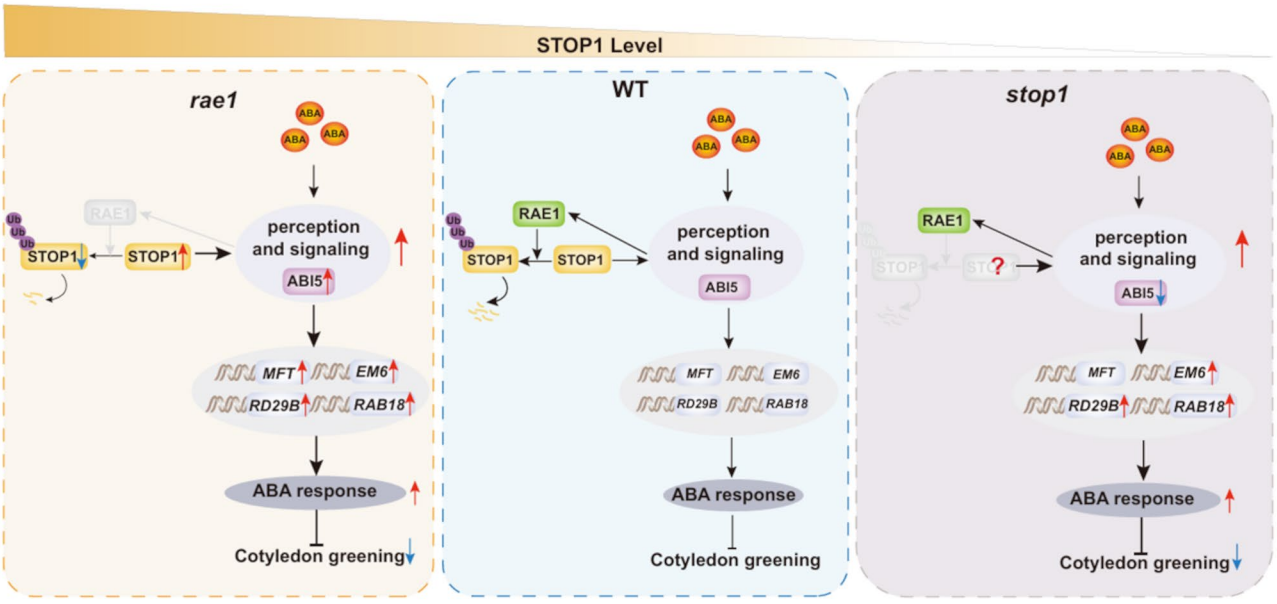

Fig. 7 A hypothetical model illustrating the RAE1-STOP1 module in regulation of ABA sensitivity in Arabidopsis early seedlings. Exogenous ABA treatment induces the expression of Arabidopsis *RAE1*, which facilitates the ubiquitination and degradation of STOP1 in wild-type plants. In the *rae1* mutant, the absence of RAE1-mediated degradation leads to STOP1 accumulation, resulting in enhanced ABA perception and signaling characterized by ABI5 upregulation. This increase in ABI5 stimulates the expression of target genes such as *MFT*, *EM6*, *RAB18*, and *RD29B*, contributing to heightened ABA sensitivity in early seedlings. Therefore, the RAE1-STOP1 module functions as a regulatory mechanism to reduce ABA sensitivity by inhibiting ABI5 elevation during the early seedling stage in Arabidopsis. In the *STOP1* dysfunctional alleles, a still unknown mediator/complimentary pathway enhances ABA perception and signaling, resulting in the activation of ABA-responsive genes (excluding *MFT*) and an increased ABA response. Notably, reduced ABI5 levels and the lack of *MFT* expression changes in the *STOP1* dysfunctional allele distinguish it from the *rae1* and *STOP1OE* lines. This reveals a possible bidirectional modulation of ABA sensitivity by STOP1 protein levels during the early seedling stage. Disrupted STOP1 protein homeostasis in both *STOP1* upregulation lines (i.e., *rae1* mutant and *STOP1* overexpression lines) and *STOP1* dysfunctional alleles confers increased ABA sensitivity

Materials and methods

Plant materials and growth conditions

In this study, we used *Arabidopsis thaliana* plants from the Columbia (*Col-0*) genetic background. T-DNA insertion lines *rae1-a* (SAIL_736_F09), *rae1-b* (SAIL_1053_H10), and *rae1-c* (SALK_103708) were obtained from the Nottingham Arabidopsis Stock Centre (NASC). Seeds of *abi5-8* (SALK_013163C) were obtained from Arashare. Double mutants *abi5-8::rae1-b* and *cark1::rae1-b*, were generated by crossing *rae1-b* with *abi5-8* and *cark1*. Other mutant lines, *pRAE1:GUS*, *stop1-2* (SALK_114108), *rae1-1* (G499A), *stop1-3* (H352Y), *rae1-1::stop1-3*, *RAE1OE1*, *STOP1OE* (*OE1* and *OE2*), *cark1* (SALK_113377), *35s ALMT1-34*, *35s ALMT1-35* and *almt1-ko* (SALK_00962) were reported previously [26, 42, 55, 57]. A DNA fragment harboring a 2.4 kb *RAE1* promoter and a 4 kb genome sequence were cloned into the *pCAMBIA1301* vector. The resulting vector was used to transform into *rae1-b* and T3 homozygous plants for complementation. All seeds were surface-sterilized by soaking with bleach (5%, v/v) for 5 min and then washed five times with sterile water. Subsequently, sterilized seeds were placed in petri dishes on half strength Murashige and Skoog (MS) solid medium (1% sucrose and 0.8% agar) and incubated at 4 °C for 48 h. Seedlings were then grown in an incubator under long-day conditions (16 h light at 23 °C / 8 h dark at 18 °C). After 7 d of growth in the petri dishes, the seedlings were transferred to soil under the same long-day conditions. Light intensity for plant growth was 120–150 μmol m^{-2} s^{-1}. Light was provided by T5 tubular LED lights (Leishi, China) at a color temperature of 6500 K.

GUS Histochemical analysis to determine *RAE1* expression

The GUS staining and experimental procedures were performed as previously described [55]. 5-d old seedlings or germinated seeds were harvested and treated with or without ABA for 3 h and incubated in freshly prepared GUS staining solution for an additional at 37 °C in darkness. Seedlings or seeds were washed three times with 70% ethanol until no green color was visible. Stained seedlings or germinated seeds were observed under a stereomicroscope (Leica, M165FC). Stained roots were observed under a fluorescence microscope (Leica, DFC420C). Root tissue was ground into a fine powder under liquid nitrogen, and then GUS activity was determined using a β-glucuronidase kit (geruisi, G0579F) according to manufacturer instructions.

Bimolecular fluorescence complementation (BiFC) assay in Arabidopsis protoplasts

The coding sequences of *RAE1* and *ASK1/ABI5* were cloned into *pSAT-cEYFP* and *pSAT-nEYFP* vectors, respectively. The resultant *RAE1-cEYFP* and *ASK1/ABI5-nEYFP* were co-transformed into Arabidopsis protoplasts with or without 10 μM ABA treatment. Protoplast preparation and transformation were performed as described previously [58]. Protoplasts were prepared from the fourth, fifth, sixth, and seventh true leaves of 3–4 week old soil-grown Arabidopsis plants. Transfected protoplasts were incubated for 16 h before the YFP signal was assayed using a Zeiss. LSM710 confocal microscope (excitation wavelength at 488 nm and emission wavelength at 500–530 nm). Images were acquired using a 40× lens with a pinhole diameter of 1 airy unit (corresponding to an optical slice of 4.37 μm). Confocal images were further processed using the ImageJ software for quantification.

STOP1 ubiquitination assay in Arabidopsis protoplasts

Protoplasts were derived from the fourth, fifth, sixth, and seventh true leaves of 3-4-week-old soil-grown wild-type (WT) and *rae1-b* Arabidopsis plants. For in vitro translation, two pHBT expression vectors containing either *35 S: STOP1-2FLAG* or *UBQ10-3HA* were co-transformed into protoplasts and subsequently incubated for 20 h with or without ABA treatment at 20 μM. Following the incubation period, protoplasts were subjected to treatment with MG132 for an additional 6 h before total protein extraction using an extraction buffer containing 50 mM Tris (pH 7.5), 150 mM NaCl, 0.1% sodium dodecyl sulfate (SDS), 1% Triton X-100, 1 mM EGTA, 1 mM DTT, 1× complete protease inhibitor cocktail, and 1 mM PMSF. Protein STOP1 was selectively enriched from the total protein extract using Anti-FLAG® M2 Magnetic Beads (Sigma-Aldrich, M8823). Subsequently, the ubiquitination status of STOP1 was assessed using an anti-HA antibody (Proteintech, 66006-2-Ig). Protoplast preparation and transformation procedures were performed as previously described [58].

Western blot assay

Abundance of the STOP1 protein was determined in 9-d old WT and *rae1-b* mutant plants. Briefly, 7-d old seedlings grown on half-strength MS solid-medium plates were transferred to new half-strength MS plates with or without 10 μM ABA for another 2 d. Control and ABA treated seedling were transferred to half strength liquid MS medium with or without 50 μM MG132 and incubated for 6 h. Seedlings (0.1 g fresh weight) were homogenized to a fine powder under liquid nitrogen before protein extraction using four volumes of extraction buffer containing 50 mM Tris pH 7.5, 150 mM NaCl, 0.1% sodium dodecyl sulfate (SDS), 1% Triton X-100, 1 mM EGTA, 1 mM DTT, 1× complete protease inhibitor cocktail, and 1 mM PMSF. Total protein in the extraction buffer was centrifuged at 12,000 g for 10 min at 4 °C to remove cell debris. The supernatant was collected, and protein concentration was measured using the Amido-black protocol for equal loading in SDS–PAGE. Proteins were blotted to a PVDF membrane (0.45 μm, Millipore) and incubated in a rabbit polyclonal antibody against STOP1 (ABclonal, A21044 with 1:500 dilution) or ACTIN (Abmart, M20009, 1:2000 dilution) antibody as an internal reference. Horseradish peroxidase (HRP) anti-rabbit IgG (H + L) (Proteintech, SA00001 at 1:2,000 dilution) was added for visualization.

ABI5 protein abundance was determined in 6 d old Arabidopsis seedlings (WT, *rae1-b*, *stop1-2* and *STOP1OE1*). 5 d old half-strength MS plate-grown seedlings were transferred to new half-strength MS plates with or without 10 μM ABA for another day. Total protein extraction and western blot were performed as previously described, using an antibody against ABI5 (Agrisera, AS121863, 1:1000 dilution) or FBA8 (PhytoAB, PHY2192S, 1:1000 dilution).

Cotyledon greening assays

Sterilized seeds were sown on half strength MS plates with or without 1 μM ABA and vernalized at 4 °C for 2 d. Plates were transferred to a growth cabinet for long-term cultivation under long day conditions (16 h of light at 23 °C, followed by 8 h of darkness at 18 °C). The percentage of seedlings with greening cotyledons (emergence of visibly green cotyledons) was determined after 7 to 9 d.

Measurement of stomatal apertures

Stomatal aperture of WT and *rae1-b* plants was measured following a previously reported method [59]. Leaves were collected from 3-week-old soil-grown Arabidopsis plants. Leaves (adaxial surface-up, abaxial surface-down) were soaked for 3 h in 10 mM MES-KOH buffer (pH 6.15) containing 50 mM KCl and 10 μM $CaCl_2$ under continuous light at 22 °C. Leaves were then transferred to the same solutions with or without 10 μM ABA and incubated for an additional 3 h. The abaxial epidermis of the leaves was sliced and placed on glass slides. Advanced upright fluorescence microscopy (OLYMPUS, BX63) was used for visualization. Images of stomata from multiple leaves were captured and stomatal apertures were calculated using the ImageJ software. Three independent experiments were performed to ensure the accuracy and reliability of the results.

Water loss measurement on detached leaves

Leaves (4th, 5th and 6th true leaves) were collected from 3-week old WT and *rae1-b* Arabidopsis plants. To prevent water loss, the leaves were stored in a weighing

dish at room temperature to ensure that they were not exposed to direct sunlight or high humidity. The initial weight (W1) and real-time weight (W2) were recorded at 15 min intervals for 2 h. The water loss rate was calculated using the following formula:

Water loss rate(W1-W2) / W1 × 100%.

Phytohormone assay by LC-MS

9-d old plate grown WT and *rae1-b* seedlings were subjected to 10 μM ABA treatment in half strength MS liquid medium for 3 h. 50 mg seedlings frozen in liquid nitrogen frozen were ground to a powder using motor and pestle. Phytohormones were extracted using 500 μL extraction solution consisting of IPA (isopropanol), H_2O, and HCl (2:1:0.002). Deuterated phytohormones were spiked in the extraction buffer as internal standard. After incubation for thirty minutes in extraction buffer, 1 ml of chloroform ($CHCl_3$) was added and incubated for another thirty minutes. The same volume supernatant was dehydrated in nitrogen gas. Dehydrated samples were solubilized by 0.1 ml methanol and filtered by 0.1 μm column. Samples were injected to a UPLC-MS for phytohormone identification and quantification. UPLC I-Class Settings: Mobile phase is A: 0.05% acetic acid in H_2O, B: 0.05% acetic acid in acetonitrile. The chromatographic column is poresell EC-120 3 μm 100 mm, with a sample loading volume of 5 μL and a flow rate of 0.3 mL/min. The column temperature is 35 °C and the sample temperature is 15 °C. Q-Exactive MS Settings: Ion Source is HESI, Spray Voltage (-) is 3000, Capillary Temperature is 320, Sheath Gas is 30, Aux Gas is 10, Spare Gas is 5, Probe Heater Temp. is 350, S-Lens RF Level is 55, FULL MS-SIM: Resolution: 70,000, AGC target is 3e6, Maximum IT is 100, Scan range is 50 to 750 m/z.

RNA deep sequencing analysis

7-d old WT and *rae1-b* Arabidopsis seedling were treated with half strength MS liquid medium containing 10 μM ABA for 3 h. 100 mg samples were frozen in liquid nitrogen. RNA was extracted from biological triplicates. RNA extraction, sample bank quality control and sequencing were completed by OE B.otech (Shanghai, China) as a service. The mRNA of poly (A) tail was enriched by Oligo (dT) magnetic beads. RNA integrity was assessed using the Agilent 2100 Bioanalyzer (Agilent Technologies, Santa Clara, CA, USA). Samples with RNA integrity Number (RIN) ≥ 7 were analyzed. The libraries were constructed using TruSeq Stranded mRNA LT Sample Prep Kit (Illumina, San Diego, CA, USA) according to the manufacturer's instructions. These libraries were then sequenced on Illumina sequencing platform (DNBSEQ-T7) and generated paired end readings of 125 bp/150 bp. Raw data (raw readings) were processed using Trimmomatic [60]. Remove readings containing poly-N and low-quality reads to obtain a clean reading. The clean reading is then mapped to the reference genome using hisat2 [61]. The FPKM [62] value of each gene was calculated using cufflinks [63], and the read counts of each gene were obtained by htseq-count [64]. DEGs were identified using the DESeq [65] R package functions Estimate Size Factors and nbinomTest P-value < 0.05 with fold change > 1.5 was set as the threshold for significantly differential expression. Hierarchical cluster analysis of DEGs was performed to explore the gene expression patterns.

RNA extraction and Q-PCR analysis

7-d old WT, *rae1-b*, *stop1-2* and *STOP1OE2* Arabidopsis seedling were treated with half strength MS liquid medium with/without 10 μM ABA for 3 h. 100 mg samples were frozen in liquid nitrogen. RNA was extracted from biological triplicates. Collected seedlings (~0.1 g) were snap frozen in liquid nitrogen and homogenized to powder using beads (2 mm) by a homogenizer. RNA was extracted using TaKaRa MiniBEST Plant RNA Extraction Kit (TaKaRa, 9767) following the manufacturer's instructions. 500ng of RNA was used for cDNA synthesis with TSINGKE Goldenstar™ RT6 cDNA Synthesis Kit Ver.2 (TSINGKE, TSK302M). Transcripts of selected genes were quantified using 2X Universal SYBR Green Fast qPCR Mix (ABclonal, RK21203) with LightCycler® 96 SW 1.1. Q-PCR data were normalized to a housekeeping gene *UBQ1 or UBQ10* before being compared across genotypes. The qRT-PCR primers used for the tested genes (*RAE1*, *ABI5*, *ABI1*, *ABI2*, *MFT*, *EM6*, *RD29B*, *RAB18 ABF1*, *ABF3*, *SNRK2.8*, and *SNRK2.3*) are provided in Data S6.

Yeast two-hybrid assay

The coding sequences of *ABI5* and *RAE1* with or without mutations were cloned into *pGADT7* (GAL-4 activation domain) and *pGBKT7* (GAL-4-binding domain) plasmids, respectively. The lithium acetate yeast transformation method was used to introduce the constructs into the yeast strain AH109 cells. Briefly, yeast cells were incubated for 6 h at room temperature in a 500 μL solution containing 600–800 ng vectors and 1 M LiAc, 1 M Tris-HCL 0.5 M EDTA (pH = 8.0) and 45% PEG4000. The transformed yeasts were plated onto a nutrient-deficient medium for the selection of positive interactions.

Abbreviations

ABA	Abscisic acid
DEGs	Differentially expressed genes
DTT	Dithiothreitol
EGTA	Ethylene glycol-bis(2-aminoethylether)-N, N,N',N'-tetraacetic acid
FPKM	Fragments Per Kilobase of exon model per Million mapped fragments
GO	Gene Ontology
PCA	Principal component analysis
PCR	Polymerase Chain Reaction
PEG	Polyethylene glycol

PMSF	Phenylmethanesulfonyl fluoride
SDS	Sodium dodecyl sulfate
TFs	Transcription Factors
YFP	Yellow fluorescent protein

Supplementary Information

The online version contains supplementary material available at https://doi.org/10.1186/s12870-025-06635-2.

Supplementary Material 1

Supplementary Material 2

Supplementary Material 3

Supplementary Material 4

Supplementary Material 5

Supplementary Material 6

Supplementary Material 7

Supplementary Material 8

Supplementary Material 9

Acknowledgements

Professor Hiroyuki Koyama (Faculty of Applied Biological Sciences, Gifu University) is thanked for providing almt1-ko (SALK_009629) and ALMT1-OE seeds. Professor Yi Wang (College of Biological Sciences, China Agricultural University) for providing STOP1OE1 and STOP1OE2 seeds. Professor Yi Yang (College of Biological Sciences, Sichuan University) for providing cark1 (SALK_113377) seeds. Professor Zhen Li (College of Biological Sciences, China Agricultural University) for assistance in the ABA contents assay in Arabidopsis.

Author contributions

L.L. designed the research; Y.Q.Z. performed plant culture and biochemical experiments; M.H. and Y.Y.L. participated in the WB and BiFC experiments. Y.Q.H. and M.M.Y. participated in the Y2H experiments. N.N.W. and C.F.H. contributed plant mutant lines, vectors and agents. L.L. and Y.Q.Z. contributing to the writing and revision of the article.

Funding

This work was supported through funding by the National Natural Science Foundation of China (31970294 and 32470258), Tianjin Natural Science Foundation (19JCYBJC24100), and Open Research Fund of State Key Laboratory of Hybrid Rice (Wuhan University KF202201) to LL and the National Natural Science Foundation of China (32070317) to NNW.

Data availability

RNA-seq data can be accessed through the following links. BioProject: https://www.ncbi.nlm.nih.gov/bioproject/PRJNA938824. GSA: https://bigd.big.ac.cn/gsa/browse/CRA019586.

Declarations

Ethics approval and consent to participate

Not applicable.

Consent for publication

Not applicable

Competing interests

The authors declare no competing interests.

Received: 22 January 2025 / Accepted: 28 April 2025
Published online: 13 May 2025

References

1. Sawaki Y, Iuchi S, Kobayashi Y, Kobayashi Y, Ikka T, Sakurai N, Fujita M, Shinozaki K, Shibata D, Kobayashi M, et al. STOP1 regulates multiple genes that protect Arabidopsis from proton and aluminum toxicities. Plant Physiol. 2009;150(1):281–94.
2. Balzergue C, Dartevelle T, Godon C, Laugier E, Meisrimler C, Teulon JM, Creff A, Bissler M, Brouchoud C, Hagege A, et al. Low phosphate activates STOP1-ALMT1 to rapidly inhibit root cell elongation. Nat Commun. 2017;8:15300.
3. Sadhukhan A, Enomoto T, Kobayashi Y, Watanabe T, Iuchi S, Kobayashi M, Sahoo L, Yamamoto YY, Koyama H. Sensitive to proton Rhizotoxicity1 regulates salt and drought tolerance of Arabidopsis thaliana through transcriptional regulation of CIPK23. Plant Cell Physiol. 2019;60(9):2113–26.
4. Sadhukhan A, Kobayashi Y, Iuchi S, Koyama H. Synergistic and antagonistic Pleiotropy of STOP1 in stress tolerance. Trends Plant Sci. 2021;26(10):1014–22.
5. Cao H, Zhang M, Zhu X, Bai Z, Ma Y, Huang CF, Yang ZB. The RAE1-STOP1-GL2-RHD6 module regulates the ALMT1-dependent aluminum resistance in Arabidopsis. Nat Commun. 2024;15(1):6294.
6. Ye JY, Tian WH, Zhou M, Zhu QY, Du WX, Zhu YX, Liu XX, Lin XY, Zheng SJ, Jin CW. STOP1 activates NRT1.1-mediated nitrate uptake to create a favorable rhizospheric pH for plant adaptation to acidity. Plant Cell. 2021;33(12):3658–74.
7. Fang Q, Zhou F, Zhang Y, Singh S, Huang CF. Degradation of STOP1 mediated by the F-box proteins RAH1 and RAE1 balances aluminum resistance and plant growth in Arabidopsis thaliana. Plant J. 2021;106(2):493–506.
8. Xu J, Zhu J, Liu J, Wang J, Ding Z, Tian H. SIZ1 negatively regulates aluminum resistance by mediating the STOP1-ALMT1 pathway in Arabidopsis. J Integr Plant Biol. 2021;63(6):1147–60.
9. Fang Q, Zhang J, Zhang Y, Fan N, van den Burg HA, Huang CF. Regulation of aluminum resistance in Arabidopsis involves the sumoylation of the zinc finger transcription factor STOP1. Plant Cell. 2020;32(12):3921–38.
10. Zhou F, Singh S, Zhang J, Fang Q, Li C, Wang J, Zhao C, Wang P, Huang CF. The MEKK1-MKK1/2-MPK4 cascade phosphorylates and stabilizes STOP1 to confer aluminum resistance in Arabidopsis. Mol Plant. 2023;16(2):337–53.
11. Jiang F, Lyi SM, Sun T, Li L, Wang T, Liu J. Involvement of cytokinins in STOP1-mediated resistance to proton toxicity. Stress Biol. 2022;2(1):17.
12. Song L, Huang SC, Wise A, Castanon R, Nery JR, Chen H, Watanabe M, Thomas J, Bar-Joseph Z, Ecker JR. A transcription factor hierarchy defines an environmental stress response network. *Science* 2016, 354(6312).
13. Zhu JK. Abiotic stress signaling and responses in plants. Cell. 2016;167(2):313–24.
14. Cutler SR, Rodriguez PL, Finkelstein RR, Abrams SR. Abscisic acid: emergence of a core signaling network. Annu Rev Plant Biol. 2010;61:61:651–79.
15. Yoshida T, Christmann A, Yamaguchi-Shinozaki K, Grill E, Fernie AR. Revisiting the basal role of ABA - roles outside of stress. Trends Plant Sci. 2019;24(7):625–35.
16. Chen K, Li GJ, Bressan RA, Song CP, Zhu JK, Zhao Y. Abscisic acid dynamics, signaling, and functions in plants. J Integr Plant Biol. 2020;62(1):25–54.
17. Ma Y, Szostkiewicz I, Korte A, Moes D, Yang Y, Christmann A, Grill E. Regulators of PP2C phosphatase activity function as abscisic acid sensors. Science. 2009;324(5930):1064–8.
18. Park SY, Fung P, Nishimura N, Jensen DR, Fujii H, Zhao Y, Lumba S, Santiago J, Rodrigues A, Chow TFF, et al. Abscisic acid inhibits type 2 C protein phosphatases via the PYR/PYL family of START proteins. Science. 2009;324(5930):1068–71.
19. Fujii H, Chinnusamy V, Rodrigues A, Rubio S, Antoni R, Park SY, Cutler SR, Sheen J, Rodriguez PL, Zhu JK. Reconstitution of an abscisic acid signalling pathway. Nature. 2009;462(7273):660–U138.
20. Umezawa T, Nakashima K, Miyakawa T, Kuromori T, Tanokura M, Shinozaki K, Yamaguchi-Shinozaki K. Molecular basis of the core regulatory network in ABA responses: sensing, signaling and transport. Plant Cell Physiol. 2010;51(11):1821–39.
21. Wang K, He JN, Zhao Y, Wu T, Zhou XF, Ding YL, Kong LY, Wang XJ, Wang Y, Li JG, et al. EAR1 negatively regulates ABA signaling by enhancing 2 C protein phosphatase activity. Plant Cell. 2018;30(4):815–34.
22. Raghavendra AS, Gonugunta VK, Christmann A, Grill E. ABA perception and signalling. Trends Plant Sci. 2010;15(7):395–401.
23. Wang XJ, Guo C, Peng J, Li C, Wan FF, Zhang SM, Zhou YY, Yan Y, Qi LJ, Sun KW, et al. ABRE-BINDING FACTORS play a role in the feedback regulation of ABA signaling by mediating rapid ABA induction of ABA co-receptor genes. New Phytol. 2019;221(1):341–55.

24. Xi W, Liu C, Hou X, Yu H. MOTHER OF FT AND TFL1 regulates seed germination through a negative feedback loop modulating ABA signaling in Arabidopsis. Plant Cell. 2010;22(6):1733–48.
25. Zhao HY, Nie KL, Zhou HP, Yan XJ, Zhan QD, Zheng Y, Song CP. ABI5 modulates seed germination via feedback regulation of the expression of the ABA receptor genes. New Phytol. 2020;228(2):596–608.
26. Zhang L, Li X, Li D, Sun Y, Li Y, Luo Q, Liu Z, Wang J, Li X, Zhang H, et al. CARK1 mediates ABA signaling by phosphorylation of ABA receptors. Cell Discov. 2018;4:30.
27. Li XY, Kong XG, Huang Q, Zhang Q, Ge H, Zhang L, Li GM, Peng L, Liu ZB, Wang JM, et al. CARK1 phosphorylates subfamily III members of ABA receptors. J Exp Bot. 2019;70(2):519–28.
28. Daspute AA, Sadhukhan A, Tokizawa M, Kobayashi Y, Panda SK, Koyama H. Transcriptional regulation of Aluminum-Tolerance genes in higher plants: clarifying the underlying molecular mechanisms. Front Plant Sci. 2017;8:1358.
29. Hou NN, You JF, Pang JD, Xu MY, Chen G, Yang ZM. The accumulation and transport of abscisic acid Insoybean (Glycine max L.) under aluminum stress. Plant Soil. 2010;330(1–2):127–37.
30. Ranjan A, Sinha R, Lal SK, Bishi SK, Singh AK. Phytohormone signalling and cross-talk to alleviate aluminium toxicity in plants. Plant Cell Rep. 2021;40(8):1331–43.
31. Kobayashi Y, Kobayashi Y, Sugimoto M, Lakshmanan V, Iuchi S, Kobayashi M, Bais HP, Koyama H. Characterization of the complex regulation of AtALMT1 expression in response to phytohormones and other inducers. Plant Physiol. 2013;162(2):732–40.
32. Fan W, Xu JM, Wu P, Yang ZX, Lou HQ, Chen WW, Jin JF, Zheng SJ, Yang JL. Alleviation by abscisic acid of al toxicity in rice bean is not associated with citrate efflux but depends on ABI5-mediated signal transduction pathways. J Integr Plant Biol. 2019;61(2):140–54.
33. Yamaji N, Huang CF, Nagao S, Yano M, Sato Y, Nagamura Y, Ma JF. A zinc finger transcription factor ART1 regulates multiple genes implicated in aluminum tolerance in rice. Plant Cell. 2009;21(10):3339–49.
34. Huang CF, Yamaji N, Mitani N, Yano M, Nagamura Y, Ma JF. A bacterial-type ABC transporter is involved in aluminum tolerance in rice. Plant Cell. 2009;21(2):655–67.
35. Arenhart RA, Bai Y, de Oliveira LF, Neto LB, Schunemann M, Maraschin Fdos S, Mariath J, Silverio A, Sachetto-Martins G, Margis R, et al. New insights into aluminum tolerance in rice: the ASR5 protein binds the STAR1 promoter and other aluminum-responsive genes. Mol Plant. 2014;7(4):709–21.
36. Vishwakarma K, Upadhyay N, Kumar N, Yadav G, Singh J, Mishra RK, Kumar V, Verma R, Upadhyay RG, Pandey M, et al. Abscisic acid signaling and abiotic stress tolerance in plants: A review on current knowledge and future prospects. Front Plant Sci. 2017;8:161.
37. Ahmed IM, Nadira UA, Cao FB, He XY, Zhang GP, Wu FB. Physiological and molecular analysis on root growth associated with the tolerance to aluminum and drought individual and combined in Tibetan wild and cultivated barley. Planta. 2016;243(4):973–85.
38. Sawaki K, Sawaki Y, Zhao CR, Kobayashi Y, Koyama H. Specific transcriptomic response in the shoots of Arabidopsis thaliana after exposure to al rhizotoxicity: - potential gene expression biomarkers for evaluating al toxicity in soils. Plant Soil. 2016;409(1–2):131–42.
39. Winter D, Vinegar B, Nahal H, Ammar R, Wilson GV, Provart NJ. An electronic fluorescent pictograph browser for exploring and analyzing large-scale biological data sets. PLoS ONE. 2007;2(8):e718.
40. Santner A, Estelle M. The ubiquitin-proteasome system regulates plant hormone signaling. Plant J. 2010;61(6):1029–40.
41. Iuchi S, Koyama H, Iuchi A, Kobayashi Y, Kitabayashi S, Kobayashi Y, Ikka T, Hirayama T, Shinozaki K, Kobayashi M. Zinc finger protein STOP1 is critical for proton tolerance in Arabidopsis and coregulates a key gene in aluminum tolerance. Proc Natl Acad Sci U S A. 2007;104(23):9900–5.
42. Wang ZF, Mi TW, Gao YQ, Feng HQ, Wu WH, Wang Y. STOP1 regulates LKS1 transcription and coordinates K(+)/NH(4)(+) balance in Arabidopsis response to Low-K(+) stress. Int J Mol Sci 2021, 23(1).
43. Stone SL, Williams LA, Farmer LM, Vierstra RD, Callis J. KEEP ON GOING, a RING E3 ligase essential for Arabidopsis growth and development, is involved in abscisic acid signaling. Plant Cell. 2006;18(12):3415–28.
44. Lee JH, Yoon HJ, Terzaghi W, Martinez C, Dai M, Li J, Byun MO, Deng XW. DWA1 and DWA2, two Arabidopsis DWD protein components of CUL4-based E3 ligases, act together as negative regulators in ABA signal transduction. Plant Cell. 2010;22(6):1716–32.
45. Li Z, Li S, Jin D, Yang Y, Pu Z, Han X, Hu Y, Jiang Y. U-box E3 ubiquitin ligase PUB8 attenuates abscisic acid responses during early seedling growth. Plant Physiol. 2023;191(4):2519–33.
46. Miura K, Lee J, Jin JB, Yoo CY, Miura T, Hasegawa PM. Sumoylation of ABI5 by the Arabidopsis SUMO E3 ligase SIZ1 negatively regulates abscisic acid signaling. Proc Natl Acad Sci U S A. 2009;106(13):5418–23.
47. Du C, Liu M, Yan Y, Guo X, Cao X, Jiao Y, Zheng J, Ma Y, Xie Y, Li H, et al. The U-box E3 ubiquitin ligase PUB35 negatively regulates ABA signaling through AFP1-mediated degradation of ABI5. Plant Cell. 2024;36(9):3277–97.
48. Seo KI, Lee JH, Nezames CD, Zhong S, Song E, Byun MO, Deng XW. ABD1 is an Arabidopsis DCAF substrate receptor for CUL4-DDB1-based E3 ligases that acts as a negative regulator of abscisic acid signaling. Plant Cell. 2014;26(2):695–711.
49. Nie K, Zhao H, Wang X, Niu Y, Zhou H, Zheng Y. The MIEL1-ABI5/MYB30 regulatory module fine tunes abscisic acid signaling during seed germination. J Integr Plant Biol. 2022;64(4):930–41.
50. Cole RN, Fang Q, Wang Z. Androgen receptor nucleocytoplasmic trafficking - A one-way journey. Mol Cell Endocrinol. 2023;576:112009.
51. Singh D, Mitra O, Mahapatra K, Raghuvanshi AS, Kulkarni R, Datta S. REPRESSOR OF UV-B PHOTOMORPHOGENESIS proteins target ABA INSENSITIVE 5 for degradation to promote early plant development. Plant Physiol 2024.
52. Zhang Y, Feng S, Chen F, Chen H, Wang J, McCall C, Xiong Y, Deng XW. Arabidopsis DDB1-CUL4 ASSOCIATED FACTOR1 forms a nuclear E3 ubiquitin ligase with DDB1 and CUL4 that is involved in multiple plant developmental processes. Plant Cell. 2008;20(6):1437–55.
53. Li Z, Zhang D, Liang X, Liang J. Receptor for activated C kinase 1 counteracts ABSCISIC ACID INSENSITIVE5-mediated Inhibition of seed germination and post-germinative growth in Arabidopsis. J Exp Bot. 2024;75(13):3932–45.
54. Ojeda-Rivera JO, Oropeza-Aburto A, Herrera-Estrella L. Dissection of root transcriptional responses to low pH, aluminum toxicity and Iron excess under Pi-Limiting conditions in Arabidopsis Wild-Type and stop1 seedlings. Front Plant Sci 2020, 11.
55. Zhang Y, Zhang J, Guo J, Zhou F, Singh S, Xu X, Xie Q, Yang Z, Huang CF. F-box protein RAE1 regulates the stability of the aluminum-resistance transcription factor STOP1 in Arabidopsis. Proc Natl Acad Sci U S A. 2019;116(1):319–27.
56. Collin A, Daszkowska-Golec A, Szarejko I. Updates on the role of ABSCISIC ACID INSENSITIVE 5 (ABI5) and ABSCISIC ACID-RESPONSIVE ELEMENT BINDING factors (ABFs) in ABA signaling in different developmental stages in plants. Cells 2021, 10(8).
57. Kobayashi Y, Lakshmanan V, Kobayashi Y, Asai M, Iuchi S, Kobayashi M, Bais HP, Koyama H. Overexpression of AtALMT1 in the Arabidopsis thaliana ecotype Columbia results in enhanced Al-activated malate excretion and beneficial bacterium recruitment. Plant Signal Behav 2013, 8(9).
58. Yoo SD, Cho YH, Sheen J. Arabidopsis mesophyll protoplasts: a versatile cell system for transient gene expression analysis. Nat Protoc. 2007;2(7):1565–72.
59. Cheong YH, Pandey GK, Grant JJ, Batistic O, Li L, Kim BG, Lee SC, Kudla J, Luan S. Two calcineurin B-like calcium sensors, interacting with protein kinase CIPK23, regulate leaf transpiration and root potassium uptake in Arabidopsis. Plant J. 2007;52(2):223–39.
60. Bolger AM, Lohse M, Usadel B. Trimmomatic: a flexible trimmer for illumina sequence data. Bioinformatics. 2014;30(15):2114–20.
61. Kim D, Langmead B, Salzberg SL. HISAT: a fast spliced aligner with low memory requirements. Nat Methods. 2015;12(4):357–60.
62. Roberts A, Trapnell C, Donaghey J, Rinn JL, Pachter L. Improving RNA-Seq expression estimates by correcting for fragment bias. Genome Biol. 2011;12(3):R22.
63. Trapnell C, Williams BA, Pertea G, Mortazavi A, Kwan G, van Baren MJ, Salzberg SL, Wold BJ, Pachter L. Transcript assembly and quantification by RNA-Seq reveals unannotated transcripts and isoform switching during cell differentiation. Nat Biotechnol. 2010;28(5):511–5.
64. Anders S, Pyl PT, Huber W. HTSeq–a Python framework to work with high-throughput sequencing data. Bioinformatics. 2015;31(2):166–9.
65. Anders S, Huber WJH. Germany: European molecular biology laboratory: differential expression of RNA-Seq data at the gene level–the DESeq package. Eur Mol Biology Lab. 2012;10:f1000research.

Publisher's note